

A comparison of central temperatures of the intracluster gas determined from X-ray and SZ measurements

Tong-Jie Zhang

Department of Astronomy, Beijing Normal University, Beijing, 100875; and National
Astronomical Observatories, Chinese Academy of Sciences, Beijing 100012, China

and

Xiang-Ping Wu

Beijing Astronomical Observatory and National Astronomical Observatories, Chinese
Academy of Sciences, Beijing 100012, China

Received June 16 2000; accepted July 26 2000

ABSTRACT

A combination of the X-ray imaging and SZ measurements of clusters permits an indirect determination of the radial temperature profiles of intracluster gas, which requires no assumption about the dynamical properties and the equation of state for clusters. A comparison of such a derived gas temperature with that given by the X-ray spectral analysis constitutes an effective probe of properties of intracluster gas. Using the available data of 31 clusters in literature, we have performed the first comparison of the central gas temperatures provided by the two methods. The good agreement between these two independent temperature estimates suggests that the distribution of intracluster gas is essentially consistent with isothermality characterized by a mean polytropic index of $\gamma = 0.9 \pm 0.1$.

Subject headings: galaxies: clusters: general — intergalactic medium — X-rays: galaxies

1. Introduction

While the X-ray spectroscopic measurement is a powerful and unique way nowadays to obtain the temperature of hot, diffuse gas contained within clusters of galaxies, it yields an emission-weighted temperature rather than the true temperature distribution. The lack of detailed information on the temperature profiles in clusters is probably the major source of uncertainties in the present determinations of the total masses and baryon fractions of clusters, which further hinders the dynamical properties of clusters from the cosmological applications such as the estimates of the cosmological parameters and the test of various models of structure formation in the universe. An independent, complementary method of measuring the distribution of intracluster gas is thus desirable. Silk & White (1978) were the first to suggest the utilization of the nonparametric reconstruction of the radial profiles of density [$n_e(r)$] and temperature [$T(r)$] of intracluster gas by combining the X-ray and SZ measurements. The basic idea is to inverse the observed X-ray and SZ temperature surface brightness profiles of clusters which have the functional forms of $n_e^2(r)T^{1/2}(r)$ and $n_e(r)T(r)$, respectively. And a simple combination of the two functions gives straightforwardly the gas density $n_e(r)$ and temperature $T(r)$. This method requires no assumption about the dynamical properties of clusters and the equation of state for intracluster gas, and can therefore be regarded as an ideal and ultimate tool to probe the gas distribution in clusters under spherical approximation.

Despite its elegant mathematical treatment further developed by Yoshikaya & Suto (1999) based on some theoretical models, the pioneering suggestion of Silk & White (1978) has not yet been put into practice to date. This has been primarily limited by the instrumental sensitivity and resolution of detecting the temperature variations of the cosmic background radiation (CBR) behind clusters. So far, the marginal detections of the radial SZ temperature distributions have been reported only for a few clusters (see

Birkinshaw 1999), which can hardly be used for the purpose of reconstructing the gas temperature profiles because of the sparse data points and the large associated uncertainties. Nevertheless, we notice that the central measured or estimated SZ effects have been available for a great number of clusters with the past two decades' efforts, and these central CBR temperature decrements in the Rayleigh-Jeans limit are usually used for setting constraints on the cosmological parameters (H_0 , Ω_M and Ω_Λ) in conjunction with the X-ray imaging and spectral measurements. Yet, another application of the central SZ data is instead to estimate the central temperature of intracluster gas when combined with the X-ray imaging observation, although this does not completely achieve the original goal of Silk & White (1978). It provides an indirect measurement of the X-ray temperature at cluster centers, which can be directly compared with the result given by the X-ray spectral analysis. Additionally, because both X-ray emission and SZ effect result from the gas distribution projected along the light of sight, a comparison of the central temperatures indicated by the two methods may also reveal valuable information about the radial temperature variations. Using the published X-ray and SZ data in literature, we present for the first time such a comparison in this paper and discuss its implications for dynamical properties of clusters. Throughout the paper we assume $H_0 = 50 \text{ km s}^{-1} \text{ Mpc}^{-1}$ and $\Omega_0 = 1$.

2. The model

The X-ray imaging observation provides a reliable measurement of the X-ray azimuthally-averaged surface brightness profile of a cluster which is usually described by the conventional β model (Cavaliere & Fusco-Femiano 1976)

$$S_x(r) = S_0 \left(1 + \frac{r^2}{r_c^2}\right)^{-3\beta+1/2}. \quad (1)$$

In the scenario of an optically-thin, thermal bremsstrahlung emission, the above form of $S_x(r)$ indicates (Cowie, Henriksen & Mushotzky 1987)

$$n_e(r)T^{1/4}(r) = n_{e0}T_0^{1/4} \left(1 + \frac{r^2}{r_c^2}\right)^{-3\beta/2}, \quad (2)$$

where n_e and T are the electron number density and temperature, respectively. If we assume an equation of state, $T(r) = T_0[n_e(r)/n_{e0}]^{\gamma-1}$, we can write the electron number density as $n_e(r) = n_{e0}(1 + r^2/r_c^2)^{-\delta}$, in which $\delta = 6\beta/(3 + \gamma)$. The central electron number density n_{e0} , temperature T_0 and the X-ray surface brightness S_0 are connected by

$$n_{e0}^2 = \left(\frac{3m_e\hbar c^2}{2^4 e^6}\right) \left(\frac{3m_e c^2}{2\pi k T_0}\right)^{1/2} \frac{4\pi^{1/2}}{\mu_e g} \frac{\Gamma(3\beta)}{\Gamma(3\beta - 1/2)} \frac{S_0(1+z)^4}{r_c}, \quad (3)$$

where $\mu_e = 2/(1 + X)$, $X = 0.768$ is the primordial hydrogen mass fraction, $g \approx 1.2$ is the average Gaunt factor, Γ is the gamma function, and z is the cluster redshift.

On the other hand, the CBR temperature decrement/increment at the cluster center predicted by the SZ effect is

$$\frac{\Delta T_{sz}}{T_{\text{CBR}}} = -4\xi(x) \int_0^{+\infty} \frac{kT(r)}{m_e c^2} \sigma_T n_e(r) dr, \quad (4)$$

$$\xi(x) = \frac{x^2 e^x}{2(e^x - 1)^2} \left(4 - x \coth \frac{x}{2}\right), \quad (5)$$

where T_{CBR} is the temperature of the present CBR, and $x = h\nu/kT_{\text{CBR}}$ is the dimensionless frequency. A straightforward computation using eqs.(2)-(5) as well as the polytropic equation of state gives

$$\begin{aligned} \left(\frac{kT_0}{m_e c^2}\right)^{3/2} = & \left(\frac{\Delta T_{sz}}{T_{\text{CBR}}}\right)^2 \left(\frac{\Gamma(3\beta'/2)}{\Gamma(3\beta'/2 - 1/2)}\right)^2 \frac{\Gamma(3\beta - 1/2)}{\Gamma(3\beta)} \\ & \cdot \frac{\sqrt{2}\alpha\mu_e g m_e c^3}{8\pi^2 \sqrt{3}(3\beta - 3/2)\xi^2 \sigma_T (1+z)^4 S_0 r_c} \end{aligned} \quad (6)$$

in which $\beta' = 3\beta\gamma/(3 + \gamma)$, and α is the fine structure constant. The above expression is often used in the determination of the Hubble constant for an isothermal gas distribution if we write $r_c = d_A(z)\theta_c$ where d_A is the angular diameter distance to the cluster at z . On

the other hand, given the Hubble constant and the polytropic index γ , all the parameters at the right-hand of eq.(6) are measurable from the X-ray imaging and SZ measurements, which will instead allow us to derive the central temperature of the X-ray emitting gas.

3. Application to X-ray clusters

Our cluster sample consists primarily of 21 nearby clusters studied extensively by Mason & Myers (2000) plus 10 high-redshift clusters with recent, reliable SZ data in the literature. Inclusion of a cluster is also subject to whether or not the good spectral temperature data are available in order to facilitate our comparison between different methods. We take the best-fit values of β , r_c and S_0 (or L_x) as well as the emission-weighted temperature data directly from the literature. For the latter, we adopt the temperature given by a single-phase (s.p.) model and the value by excluding the cooling flows (c.l.) (White 2000), respectively. Since the X-ray spectrum is always observed over a finite bandpass, we assume an optically-thin, thermal bremsstrahlung emission model with the metal abundances of 30% solar to convert the observed S_0 (or L_x) over the corresponding energy band into the bolometric value. We use the central SZ decrement/increment of ΔT_{sz} after the correction of the finite beam in each observation. All the input data of the X-ray and SZ measurements are summarized in Table 1.

For an isothermal gas distribution, the jointly determined central temperature, T_{est} , from the X-ray imaging and SZ measurements (eq.[6]) can be directly compared with the X-ray spectral result, T_{spec} . We display in Fig.1 our derived T_{est} versus the observed T_{spec} (s.p. model) for the 31 clusters in Table 1. A glimpse of Fig.1 reveals that the two sets of data are roughly consistent with each other. The best-fit T_{spec} - T_{est} relation reads

$$T_{est} = 10^{-0.22 \pm 0.18} T_{spec}^{1.22 \pm 0.20}, \quad \text{s.p. model}; \quad (7)$$

$$T_{set} = 10^{-0.36 \pm 0.26} T_{spec}^{1.29 \pm 0.29}, \text{ c.l. corrected,} \quad (8)$$

in which the error bars are the 90% confidence limits which have taken the measurement uncertainties into account. We have also tested the dependence of the best-fit T_{spec} - T_{est} relation on the Hubble constant by adopting a larger value of $H_0 = 75 \text{ km s}^{-1} \text{ Mpc}^{-1}$. This only leads to a minor modification to the above results. For instance, the best-fit relation for the s.p. model now reads $T_{est} = 10^{-0.34 \pm 0.11} T_{spec}^{1.22 \pm 0.12}$.

EDITOR: PLACE FIGURE 1 HERE.

If the intracluster gas deviates from isothermality, our comparison of T_{est} and T_{spec} becomes to be a little complex because we need to recover the central temperature from the emission-weighted spectral fit. On the other hand, we can place a useful constraint on the polytropic index γ if we demand that our derived central temperature from eq.(6) identify the spectral value after a proper correction to the emission-weighted temperature \bar{T} predicted by

$$\frac{dE}{d\nu} \propto \bar{T}^{-1/2} g_{ff}(\bar{T}, \nu) \exp(-h\nu/k\bar{T}) \int n_e^2 dV, \quad (9)$$

where g_{ff} is the Gaunt factor of the free-free emission, ν is the X-ray observing frequency, and the integration is performed over the whole cluster volume if we neglect the finite detection aperture. This compares with the theoretically expected spectrum for the hot intracluster gas

$$\frac{dE}{d\nu} \propto \int n_e^2 T^{-1/2} g_{ff}(T, \nu) \exp(-h\nu/kT) dV. \quad (10)$$

For each cluster with the reported $\bar{T} = T_{spec}$, we use the Monte Carlo simulations over the typical energy band 0.5 - 10 keV to obtain the central temperature T_0 and the corresponding γ with the restriction of eq.(6). The resultant γ value for each cluster is listed in Table 1, and a combined analysis of the results among the 31 clusters yields

$$\langle \gamma \rangle = 0.91 \pm 0.14, \text{ s.p. model; } \quad (11)$$

$$\langle \gamma \rangle = 0.93 \pm 0.14, \text{ c.l. corrected,} \quad (12)$$

which indicates that clusters are essentially consistent with isothermality at 90% significance level.

4. Discussion and conclusions

Our joint analysis of the indirect and direct temperature measurements from the X-ray and SZ observations provides a useful clue to resolving the temperature profile discrepancy raised in recent years particularly by Markevitch et al. (1998), Irwin, Bregman & Evrard (1999), White (2000) and Irwin & Bregman (2000). Markevitch et al. (1998) claimed a significant temperature decline with increasing radius represented by a polytropic index of 1.2-1.3, while the other investigators have essentially detected an isothermal temperature profile. Our present study gives an independent yet convincing evidence for the assumption of isothermality. The advantage of our algorithm over the previous analysis is that we have obtained the central temperatures of clusters without utilizing the X-ray spectral data, while a combination of both has allowed us to set a valuable constraint on the radial temperature profiles of the hot X-ray emitting gas.

A joint determination of the central temperature of intracluster gas from the X-ray imaging and SZ measurements can be used at present as an independent and complementary method to examine the reliability and accuracy of the temperature measurement provided by the conventional X-ray spectral analysis, although our ultimate goal is to obtain the detailed radial profiles of electron number density and temperature when the SZ surface brightness can be precisely mapped (Silk & White, 1978; Yoshikawa & Suto 1999). Yet, we should point out that it may not be easy to identify the temperature structure of the hot gas from such a combined analysis, in the sense that the dominant component in both S_x and ΔT_{sz} is characterized by the sharp decrease of the electron number density with

outward radius, while it is unlikely that the temperature profiles can demonstrate a similar variation. An accurate measurement of S_x and ΔT_{sz} at outermost radii will thus be needed if one wants to apply the present technique to the reconstruction of temperature profiles of intracluster gas. Alternatively, the present technique requires that the X-ray surface brightness is well represented by the β model. Presence of cooling flows in the central regions of many X-ray clusters may yield an underestimate of the β parameter and the core radius r_c and an overestimate of the central surface brightness S_0 , which will in turn affect our estimate of T_{est} through eq.(6). Indeed, an examination of Fig.1 reveals that all the massive cooling flow clusters with $\dot{M} > 600 M_\odot \text{ yr}^{-1}$ (A478, A1835, A2204 and Zw3146) demonstrate rather large scatters around the $T_{est} = T_{spec}$ relation. Therefore, the present method is most applicable to morphologically simple clusters without cooling flows.

This work was supported by the National Science Foundation of China, under Grant 19725311.

REFERENCES

Arnaud, M., & Evrard, A. E., 1999, MNRAS, 305, 631

Birkinshaw, M., 1999, Phys. Rep., 310, 97

Cavaliere, A., & Fusco-Femiano, R., 1976, A&A, 49, 137

Cooray, A. R., 1999, MNRAS, 307, 841

Cowie, L. L., Henriksen, M., & Mushotzky, R. F., 1987, ApJ, 317, 593

Ettori, S., & Fabian, A. C., 1999, MNRAS, 305, 834

Irwin, J. A., & Bregman, J. N., 2000, ApJ, in press

Irwin, J. A., Bregman, J. N., & Evrard, A. E., 1999, ApJ, 519, 518

Markevitch, M., Vikhlinin, A., Forman, W. R., & Sarazin, C. L., 1998, ApJ, 527, 545

Mason, B. S., & Myers, S. T., 2000, ApJ, in press

Mohr, J. J., Mathiesen, B., & Evrard, A. E., 1999, ApJ, 517, 627

Reese, E.D., et al., 2000, ApJ, 533, 38

Rizza, E., & Burns, J. O., 1998, MNRAS, 301, 328

Silk, J., & White, S. D. M., 1978, ApJ, 226, L103

White, D. A., 2000, MNRAS, 312, 663

Wu, X.-P., Xue, Y.-J., & Fang, L.-Z., 1999, ApJ, 524, 22

Yoshikawa, K., & Suto, Y., 1999, ApJ, 513, 549

Fig. 1.— The derived central temperatures are plotted against the spectral results (single-phase model) for a sample of 31 clusters. Solid line shows the best-fit relation, and dotted line indicates $T_{est} = T_{spec}$. The high-redshift ($z > 0.1$) and low-redshift ($z < 0.1$) clusters are represented by the filled squares and triangles, respectively. The marked clusters are the massive cooling flow ones with $\dot{M} > 600 M_{\odot} \text{ yr}^{-1}$ (White 2000).

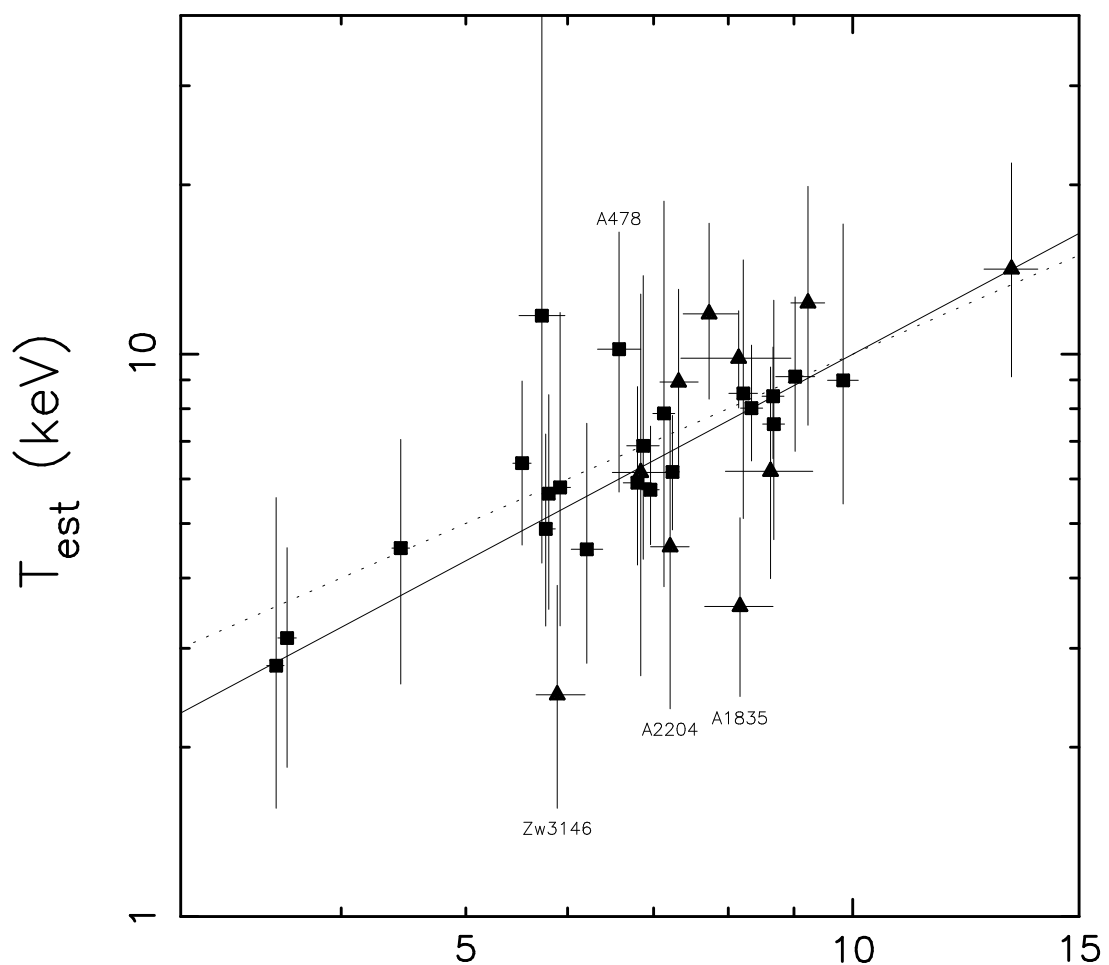


Table 1. Cluster Sample

cluster	z	β	r_c (Mpc)	L_x (10^{44} erg s $^{-1}$)	ΔT_{sz0} (mK)	T_x^a (kev)	T_x^b (kev)	T_{est} (kev)	γ^a	γ^b
A85	0.0518	$0.600^{+0.050}_{-0.050}$	$0.169^{+0.043}_{-0.043}$	$16.00^{+1.11}_{-1.11}$	$-0.50^{+0.06}_{-0.07}$	$5.92^{+0.11}_{-0.11}$	$6.74^{+0.50}_{-0.50}$	$5.80^{+6.06}_{-2.51}$	0.98	0.8
A399	0.0751	$0.742^{+0.042}_{-0.042}$	$0.500^{+0.052}_{-0.052}$	$13.32^{+1.62}_{-1.62}$	$-0.33^{+0.04}_{-0.04}$	$6.80^{+0.17}_{-0.17}$	$9.55^{+1.92}_{-0.96}$	$5.91^{+2.85}_{-1.69}$	0.87	0.8
A401	0.0748	$0.636^{+0.047}_{-0.047}$	$0.260^{+0.047}_{-0.047}$	$21.58^{+2.00}_{-2.00}$	$-0.61^{+0.08}_{-0.08}$	$8.68^{+0.17}_{-0.17}$	$10.68^{+1.11}_{-0.94}$	$7.51^{+4.96}_{-2.83}$	0.87	0.8
A478	0.0900	$0.638^{+0.014}_{-0.014}$	$0.135^{+0.020}_{-0.020}$	$26.20^{+3.34}_{-3.34}$	$-1.19^{+0.29}_{-0.23}$	$6.58^{+0.26}_{-0.25}$	$7.42^{+0.71}_{-0.54}$	$10.20^{+6.29}_{-4.52}$	1.20	1.19
A754	0.0528	$0.713^{+0.120}_{-0.120}$	$0.463^{+0.093}_{-0.093}$	$18.82^{+1.43}_{-1.43}$	$-0.54^{+0.06}_{-0.08}$	$9.83^{+0.27}_{-0.27}$	$12.85^{+1.77}_{-1.35}$	$8.98^{+8.05}_{-3.57}$	0.87	0.8
A780	0.0522	$0.629^{+0.028}_{-0.028}$	$0.137^{+0.032}_{-0.032}$	$9.76^{+0.82}_{-0.82}$	$-0.26^{+0.05}_{-0.08}$	$3.56^{+0.05}_{-0.06}$	$4.49^{+0.41}_{-0.37}$	$2.79^{+2.77}_{-1.23}$	0.86	0.8
A1651	0.0825	$0.712^{+0.036}_{-0.036}$	$0.271^{+0.045}_{-0.045}$	$15.40^{+1.81}_{-1.81}$	$-0.38^{+0.06}_{-0.08}$	$6.21^{+0.18}_{-0.17}$	$7.15^{+0.84}_{-0.62}$	$4.50^{+3.04}_{-1.68}$	0.84	0.8
A1656	0.0232	$0.670^{+0.003}_{-0.003}$	$0.362^{+0.004}_{-0.004}$	$16.67^{+0.43}_{-0.43}$	$-0.52^{+0.07}_{-0.08}$	$8.67^{+0.17}_{-0.17}$	$10.03^{+0.89}_{-0.81}$	$8.42^{+1.87}_{-1.90}$	0.91	0.8
A1795	0.0616	$0.698^{+0.017}_{-0.017}$	$0.210^{+0.027}_{-0.027}$	$20.85^{+1.21}_{-1.21}$	$-0.59^{+0.12}_{-0.13}$	$5.80^{+0.07}_{-0.07}$	$7.26^{+0.51}_{-0.40}$	$5.65^{+2.82}_{-2.13}$	0.91	0.8
A2029	0.0767	$0.601^{+0.030}_{-0.030}$	$0.109^{+0.011}_{-0.011}$	$34.23^{+2.42}_{-2.42}$	$-1.21^{+0.25}_{-0.28}$	$8.22^{+0.21}_{-0.21}$	$8.22^{+0.58}_{-0.20}$	$8.51^{+6.18}_{-3.41}$	1.03	1.0
A2142	0.0899	$0.635^{+0.012}_{-0.012}$	$0.216^{+0.016}_{-0.016}$	$49.80^{+3.22}_{-3.22}$	$-1.18^{+0.14}_{-0.19}$	$9.02^{+0.32}_{-0.31}$	$10.96^{+2.56}_{-1.58}$	$9.12^{+3.52}_{-2.40}$	1.00	0.8
A2255	0.0800	$0.723^{+0.015}_{-0.015}$	$0.532^{+0.015}_{-0.015}$	$10.16^{+0.45}_{-0.45}$	$-0.31^{+0.08}_{-0.17}$	$6.87^{+0.20}_{-0.20}$	$7.76^{+1.01}_{-1.01}$	$6.87^{+6.92}_{-2.55}$	0.99	0.8
A2256	0.0601	$0.847^{+0.024}_{-0.024}$	$0.520^{+0.020}_{-0.020}$	$15.04^{+0.66}_{-0.66}$	$-0.37^{+0.05}_{-0.05}$	$6.96^{+0.11}_{-0.11}$	$8.69^{+1.06}_{-1.06}$	$5.74^{+1.70}_{-1.16}$	0.85	0.8
A2597	0.0852	$0.626^{+0.018}_{-0.018}$	$0.063^{+0.004}_{-0.004}$	$12.67^{+1.48}_{-1.48}$	$-0.47^{+0.11}_{-0.08}$	$3.63^{+0.06}_{-0.06}$	$3.91^{+0.27}_{-0.22}$	$3.13^{+1.40}_{-1.29}$	0.88	0.8
A3112	0.0703	$0.560^{+0.008}_{-0.008}$	$0.057^{+0.005}_{-0.005}$	$12.09^{+0.99}_{-0.99}$	$-0.52^{+0.13}_{-0.11}$	$4.45^{+0.07}_{-0.07}$	$4.69^{+0.27}_{-0.26}$	$4.52^{+2.53}_{-1.93}$	1.01	0.9
A3158	0.0590	$0.649^{+0.018}_{-0.018}$	$0.264^{+0.015}_{-0.015}$	$9.52^{+0.61}_{-0.61}$	$-0.29^{+0.05}_{-0.05}$	$5.77^{+0.10}_{-0.05}$	$8.33^{+1.43}_{-0.95}$	$4.89^{+2.32}_{-1.61}$	0.87	0.8
A3266	0.0594	$0.942^{+0.020}_{-0.020}$	$0.796^{+0.025}_{-0.025}$	$13.46^{+0.53}_{-0.53}$	$-0.38^{+0.05}_{-0.05}$	$8.34^{+0.17}_{-0.16}$	$9.69^{+0.97}_{-0.92}$	$8.02^{+2.36}_{-1.56}$	0.87	0.8
A3558	0.0482	$0.550^{+0.006}_{-0.006}$	$0.206^{+0.005}_{-0.005}$	$10.91^{+0.96}_{-0.96}$	$-0.31^{+0.04}_{-0.05}$	$5.53^{+0.09}_{-0.09}$	$6.60^{+0.50}_{-0.50}$	$6.40^{+2.56}_{-1.82}$	1.08	0.9
A3571	0.0379	$0.669^{+0.009}_{-0.009}$	$0.225^{+0.011}_{-0.011}$	$14.82^{+0.99}_{-0.99}$	$-0.49^{+0.05}_{-0.05}$	$7.24^{+0.09}_{-0.09}$	$8.12^{+0.42}_{-0.39}$	$6.17^{+1.61}_{-1.30}$	0.87	0.8
A3667	0.0552	$0.589^{+0.051}_{-0.051}$	$0.376^{+0.084}_{-0.084}$	$18.57^{+3.44}_{-3.44}$	$-0.43^{+0.07}_{-0.08}$	$7.13^{+0.14}_{-0.14}$	$8.11^{+0.82}_{-0.73}$	$7.85^{+10.87}_{-3.99}$	1.09	0.95
A3921	0.0960	$0.541^{+0.031}_{-0.031}$	$0.190^{+0.033}_{-0.033}$	$8.98^{+1.25}_{-1.25}$	$-0.42^{+0.12}_{-0.14}$	$5.73^{+0.24}_{-0.23}$	$9.96^{+7.83}_{-7.83}$	$11.71^{+35.15}_{-7.46}$	0.70	1.00
A665	0.1820	$0.740^{+0.032}_{-0.032}$	$0.490^{+0.057}_{-0.057}$	$34.06^{+5.32}_{-5.32}$	$-0.91^{+0.09}_{-0.09}$	$7.73^{+0.41}_{-0.35}$	$7.90^{+1.45}_{-0.52}$	$11.79^{+5.30}_{-3.48}$	0.70	1.20
A773	0.1970	$0.780^{+0.033}_{-0.033}$	$0.303^{+0.035}_{-0.035}$	$28.61^{+4.77}_{-4.77}$	$-0.67^{+0.10}_{-0.10}$	$8.63^{+0.68}_{-0.67}$	$8.63^{+2.30}_{-0.64}$	$6.19^{+3.30}_{-2.20}$	0.83	0.8
A1413	0.1430	$0.670^{+0.029}_{-0.029}$	$0.210^{+0.024}_{-0.024}$	$29.38^{+3.71}_{-3.71}$	$-0.96^{+0.11}_{-0.11}$	$7.32^{+0.26}_{-0.24}$	$8.00^{+1.28}_{-0.86}$	$8.92^{+4.12}_{-2.83}$	1.14	1.00
A1689	0.1810	$0.650^{+0.040}_{-0.020}$	$0.131^{+0.022}_{-0.022}$	$45.45^{+7.28}_{-7.28}$	$-1.87^{+0.32}_{-0.32}$	$9.23^{+0.28}_{-0.28}$	$9.48^{+1.36}_{-0.52}$	$12.33^{+7.35}_{-4.86}$	1.17	1.10
A1835	0.2520	$0.720^{+0.031}_{-0.031}$	$0.090^{+0.010}_{-0.010}$	$85.35^{+11.67}_{-11.67}$	$-1.34^{+0.15}_{-0.15}$	$8.17^{+0.50}_{-0.50}$	$8.86^{+4.93}_{-4.93}$	$3.56^{+1.56}_{-1.10}$	0.77	0.70
A2163	0.2010	$0.650^{+0.028}_{-0.028}$	$0.360^{+0.042}_{-0.042}$	$107.71^{+15.74}_{-15.74}$	$-1.93^{+0.28}_{-0.28}$	$13.29^{+0.64}_{-0.64}$	$13.28^{+0.75}_{-0.60}$	$14.17^{+7.72}_{-5.05}$	1.06	1.00
A2204	0.1520	$0.660^{+0.028}_{-0.028}$	$0.120^{+0.014}_{-0.014}$	$47.80^{+5.17}_{-5.17}$	$-0.96^{+0.28}_{-0.28}$	$7.21^{+0.25}_{-0.25}$	$8.18^{+1.08}_{-1.08}$	$4.54^{+3.39}_{-2.20}$	0.82	0.8
A2218	0.1710	$0.650^{+0.080}_{-0.050}$	$0.226^{+0.080}_{-0.050}$	$17.97^{+1.64}_{-1.64}$	$-0.52^{+0.15}_{-0.15}$	$6.84^{+0.34}_{-0.34}$	$8.87^{+3.75}_{-1.74}$	$6.16^{+6.63}_{-3.48}$	0.88	0.8
Cl0016	0.5455	$0.749^{+0.024}_{-0.018}$	$0.311^{+0.018}_{-0.015}$	$52.00^{+2.00}_{-2.00}$	$-1.24^{+0.10}_{-0.10}$	$8.15^{+0.80}_{-0.80}$	$8.03^{+1.05}_{-1.05}$	$9.83^{+2.11}_{-1.81}$	1.17	1.13
Zw3146	0.2910	$0.740^{+0.032}_{-0.032}$	$0.070^{+0.008}_{-0.008}$	$45.74^{+7.78}_{-7.78}$	$-0.86^{+0.14}_{-0.14}$	$5.89^{+0.30}_{-0.22}$	$7.63^{+2.63}_{-1.30}$	$2.48^{+1.40}_{-0.92}$	0.77	0.73

^aSingle-phase model^bCooling-flow corrected

References. — Listed in order, are sources for the X-ray surface brightness profile (β and r_c), the X-ray bolometric luminosity (L_x), the central decrement, and the X-ray spectral temperature (T_{spec}), respectively: (1)Mason & Myers 2000; (2)Wu et al. 1999; (3)White 2000; (4)Ettori (5)Cooray 1999; (6)Rizza & Burns 1998; (7)Mohr et al. 1999; (8)Birkinshaw 1999; (9)Arnaud et al. 1999; (10)Reese et al. 2000.